LASER INTERFEROMETER GRAVITATIONAL WAVE OBSERVATORY
- LIGO -
CALIFORNIA INSTITUTE OF TECHNOLOGY
MASSACHUSETTS INSTITUTE OF TECHNOLOGY

**Technical Note** **LIGO-T1000276-4** 2011/12/27

# Output Mode Cleaner Design

S J Waldman

**California Institute of Technology**
**LIGO Project, MS 18-34**
**Pasadena, CA 91125**
Phone (626) 395-2129
Fax (626) 304-9834
E-mail: info@ligo.caltech.edu

**Massachusetts Institute of Technology**
**LIGO Project, Room NW22-295**
**Cambridge, MA 02139**
Phone (617) 253-4824
Fax (617) 253-7014
E-mail: info@ligo.mit.edu

**LIGO Hanford Observatory**
**Route 10, Mile Marker 2**
**Richland, WA 99352**
Phone (509) 372-8106
Fax (509) 372-8137
E-mail: info@ligo.caltech.edu

**LIGO Livingston Observatory**
**19100 LIGO Lane**
**Livingston, LA 70754**
Phone (225) 686-3100
Fax (225) 686-7189
E-mail: info@ligo.caltech.edu

http://www.ligo.caltech.edu/

# 1 Introduction

The aLIGO Output Mode Cleaner (OMC) enables the DC readout sensing scheme of the interferometer's differential arm length. The OMC is a short $\approx 1\ m$ long cavity used to isolate the fundamental DC carrier mode and its audio frequency phase sidebands from the RF fields and higher order spatial modes. The OMC integrates the DC readout photodiodes (DCPDs), quadrant photodiodes (QPDs), and length actuators required to keep the filter cavity resonant with the carrier.

The aLIGO OMC design derives from that used for Enhanced LIGO (eLIGO) with several significant changes based on our extensive operating experience. The similarities and difference are listed in Table 1:

| **Similarities:** |
|---|
| OMC consists of a 4-mirror cavity with two curved and two flat mirrors |
| Total length $\approx 1\ m$, with a $\approx 500\ \mu m$ waist size |
| Two DCPDs and two QPDs mounted directly to breadboard |
| "Tombstones" on "breadboard" UV epoxy construction |

| **Differences:** |
|---|
| A single, long throw PZT stack actuator will replace the short throw PZT and heater combination |
| Super polished, coated tombstones will replace the multi-element mirror and tombstone design |
| The photodiode preamplifiers will be removed from the suspended breadboard |
| If possible, the breadboard design will be made stiffer to move resonant frequencies higher |

Table 1: OMC design.

The most significant difference between the eLIGO and aLIGO OMCs is the RF sideband frequencies. For eLIGO, the RF sidebands were at 24.5 and 61 MHz while for aLIGO, the frequencies are 9 and 45 MHz. Furthermore, the distribution of light at the AntiSymmetric (AS) port is different. For the starting AS port powers, we use the numbers from §2.1 of Ref. [1] – calculated for the 125 W, NS/NS tuning – reproduced here in Table 2.

| Frequency [MHz] | -47 | -9.4 | 0 | 9.4 | 47 | Total |
|---|---|---|---|---|---|---|
| Power [mW] | 64 | 0.16 | 82 | 0.16 | 100 | 250 |

Table 2: Power at the AS port derived from Ref. [1] for Mode 2: 125 W input power, NS/NS tuning.

# References

[1] **T070247-v1** ISC group; *AdvLIGO Interferometer Sensing and Control Conceptual Design*

[2] **T0900511-v3** L. Barsotti and M. Evans; *Modeling of Alignment Sensing and Control for Advanced LIGO*

[3] **T1000317** K. Kawabe; *Mode Matching Telescope for Advanced LIGO Output Mode Cleaners*

# 2 Cavity math

We require a few functions to calculate an OMC's transmission. First, we model the four-mirror cavity as a symmetric, lossless linear cavity of length $L$, with two curved mirrors having radius of curvature, $R$, and power transmission, $T$. Then various appropriate equations and symbol definitions are:

| | |
|---|---|
| g-factor: | $g = 1 - L/R$ |
| Free Spectral Range: | $FSR = c/2L$ |
| One-way Gouy phase | $\phi_G = \arccos(g)$ |
| Finesse | $\mathcal{F} \approx \pi/T$ |
| Airy Fringe | $P(\delta f) = \left(1 + \frac{4\mathcal{F}^2}{\pi^2}\sin^2[\pi\delta f/FSR]\right)^{-1}$ |
| TEM00 power overlap | $P_0(\omega_1) = 4\omega_0^2\omega_1^2/\left(\omega_0^2 + \omega_1^2\right)^2$ |
| 1-D HOM field overlap | $\kappa_n(\omega_1) = \sqrt{\frac{2\alpha}{1+\alpha^2}\left(\frac{\alpha^2-1}{\alpha^2+1}\right)^n \prod_{i=1}^{n/2}\frac{2i-1}{2i}} \quad \forall n \in 2, 4, 6, \ldots$ |
| HOM power | $P_{m,n}(\omega_1) = (\kappa_m(\omega_1)\kappa_n(\omega_1))^2$ |
| Effect of astigmatism | $R'(\theta) = R\cos(\theta), \quad \text{or} \quad R/\cos(\theta)$ |

The g-factor equation assumes a linear symmetric cavity. The TEM00, 1-D HOM field overlap, and HOM power equations assume that the incoming beam waist is co-located with the cavity waist but is of the incorrect radius. The simplest math assumes the cavity consists of two identical curved optics. For the bowtie configuration described below, the folded four mirror cavity has two flat mirrors followed by two curved optics. The resulting asymmetry generates two different waist sizes. Consequently, the Gouy phase is calculated for each waist of the asymmetric cavity and summed.

# 3 OMC parameter selection

In Figures 1 and 2, the spacing of higher order spatial and RF modes was calculated for a symmetric linear cavity with lengths between 0.4 and 0.75 m and for mirrors of curvature from 0.75 to 3.5 m. The plot color shows the distance of the closest mode to the carrier, normalized by the cavity linewidth. The spacing was calculated for all modes up to $8^{\text{th}}$ order. To accomodate the reduced amplitude relative to the carrier and 45 MHz of the 9 MHz sideband, Figure 2 adds 10 linewidths to sideband spacing. In both cases, the largest region of distant spacing is located near $R = 2.5\ m$ and $L = 0.57\ m$.

The bowtie cavity spacing shown in Figure 3 uses a modified calculation for the Gouy phase appropriate for the asymmetric geometry. The region of distant spacing is very similar to the symmetric cavity.

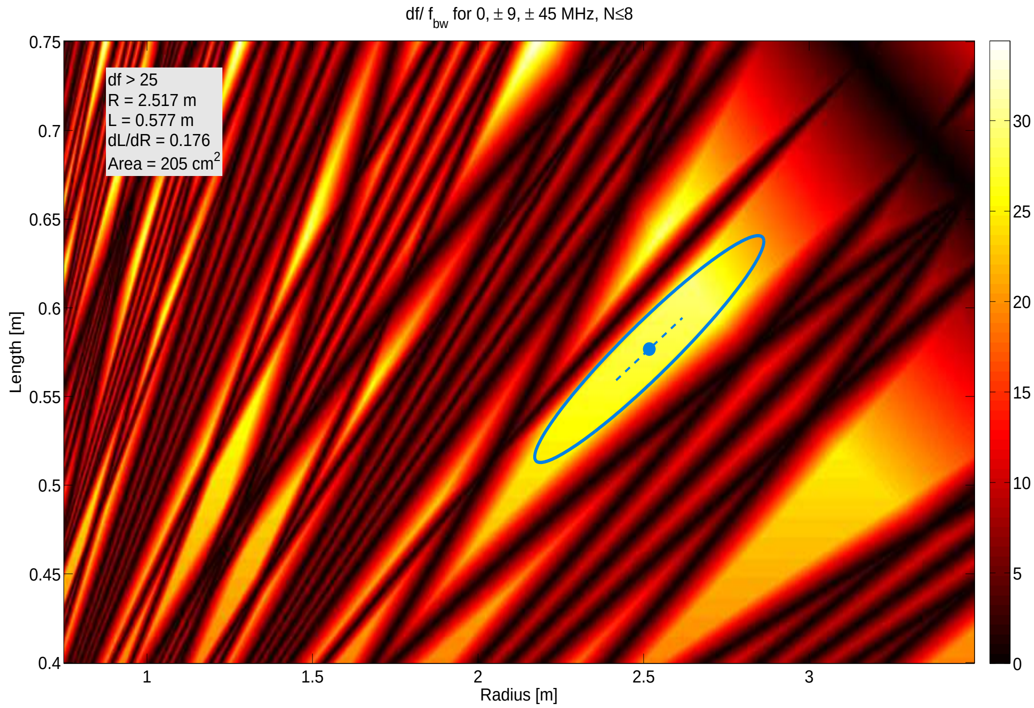


Figure 1: The spacing to the nearest mode for all mode orders up to 8. Includes 0, 9 and 45 MHz sidebands. The spacing is normalized by the cavity bandwidth for a finesse of 400.

### 3.1 Approximations

We have neglected two factors in this analysis that we believe to be relatively insignificant. First, we have neglected to include the round trip loss in the OMC in the analysis of the transmitted light. This will reduce both the transmission and the finesse. However, we believe the excess loss observed in the eLIGO OMCs (about 60 ppm roundtrip) was due to construction techniques that will be avoided for aLIGO. In particular, the use of monolithic tombstones, AR surface bonding, and not heater element should reduce the loss to negligible levels for moderate finesse. Second, the OMC has a folded design that can lead to astigmatism. This effect is minimized by keeping the angle of incidence (AOI) onto each mirror small. The target 4° AOI shifts the Gouy phase by less than 1%, with a corresponding shift in the HOM frequencies.

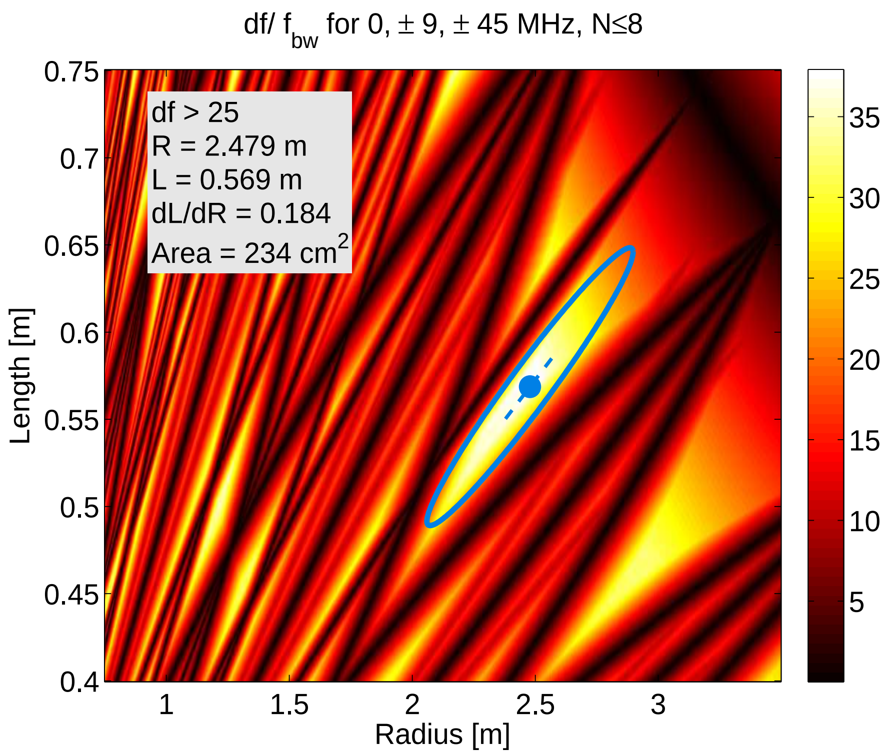


Figure 2: The spacing to the nearest mode for all mode orders up to 8. Includes 0, 9 and 45 MHz sidebands. The 9 MHz sideband spacing has been increased by 10 linewidths to account for the lower power. The spacing is normalized by the cavity bandwidth for a finesse of 400.

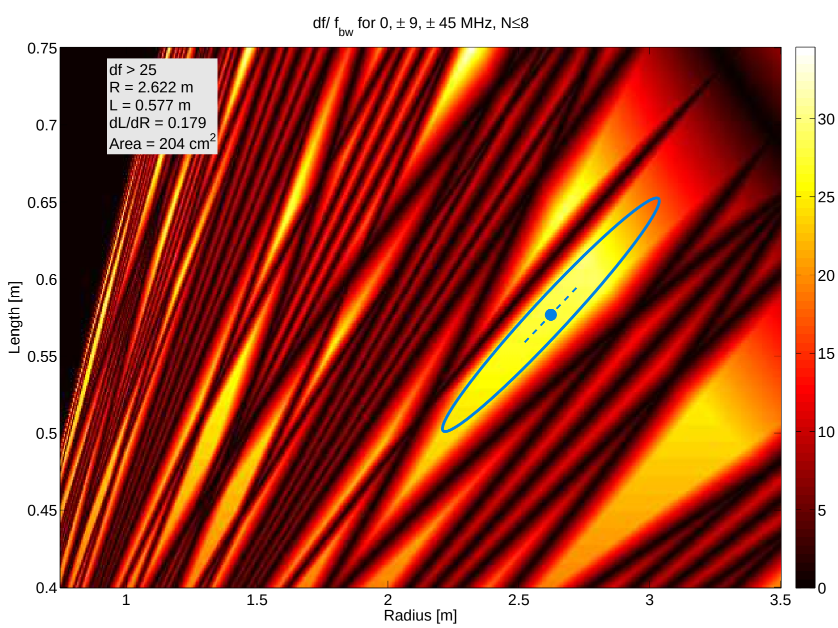


Figure 3: The spacing of the nearest mode for the asymmetric bowtie configuration.

# 4 Proposed design

The two mode cleaner designs presented here have a mirror radius of curvature of R=2.5 m and a round trip length of $\approx 1.14\ m$. Two designs fit onto the breadboard and match the HAM6 layout: an "asymmetric bowtie" design and a *sans* beam splitter design in which the beam splitter function is served by two output couplers.

Figure 4 and Figure 5 shows how the two aLIGO OMC designs fit into the current OMC footprint.

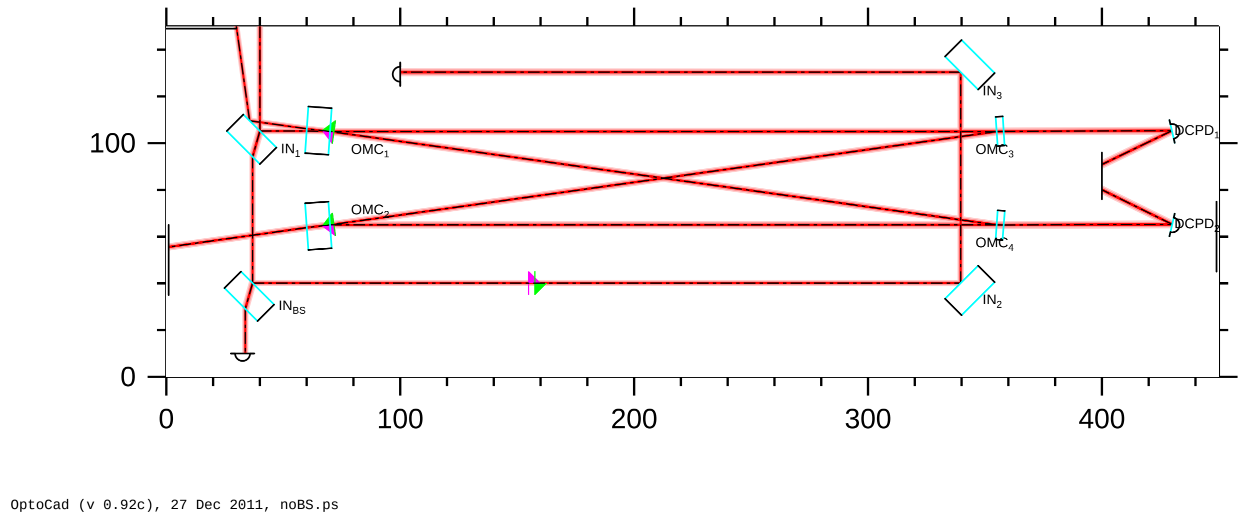


Figure 4: Schematic layout of L=1.14 m, R=2.5 m with no output Beam splitter.

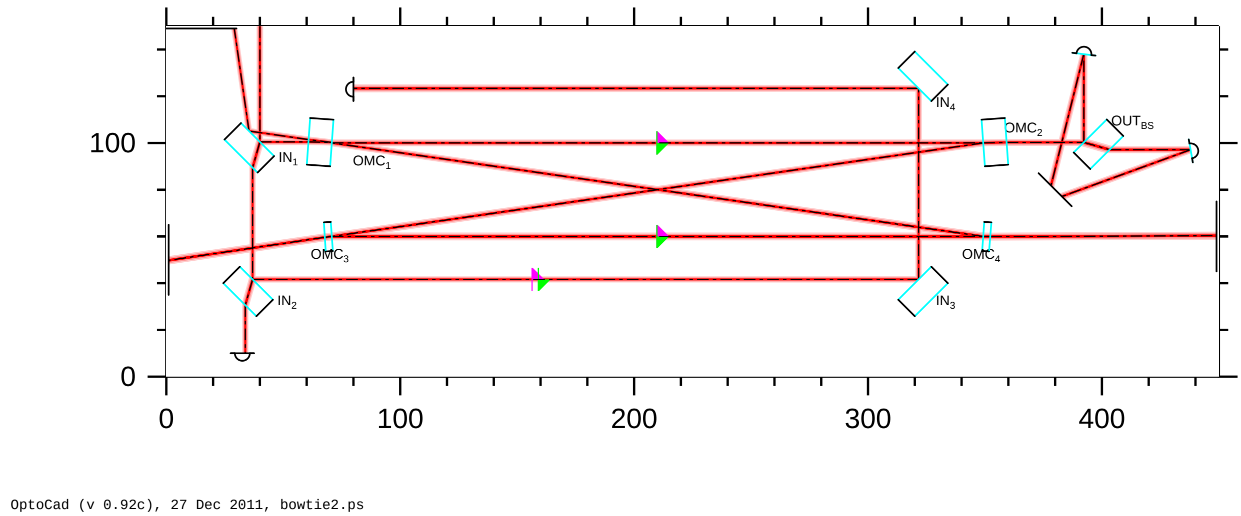


Figure 5: Schematic layout of L=1.14 m, R=2.5 m bowtie configuration with an output Beam splitter. Note that OMC1 and OMC2 are both flat optics.

There are several major differences between these layouts and eLIGO:

**No suspension interference** As described in §4.3, the suspension interfaces only to the "dark side" of the bread board and no stay-clear zones are required

**Reduced EQ stop interference** These layouts include a 1 inch by 1 inch stay clear zone at each corner for the earthquake stops. There are no EQ stops interior to the bread board.

**Input position adjusted** The input position has been adjusted to be closer to the edge of the board. This is need for the HAM6 table layout.

## 4.1 Numeric modeling

Sam Barnum has completed a finite element analysis of the breadboard, studying the displacement of the OMC mirrors as a function of the tombstone dimensions. A sample output is shown in Figure 6. The modeling has led to a selection of a tombstone that is 20 mm x 10 mm x 23 mm (WxDxH).

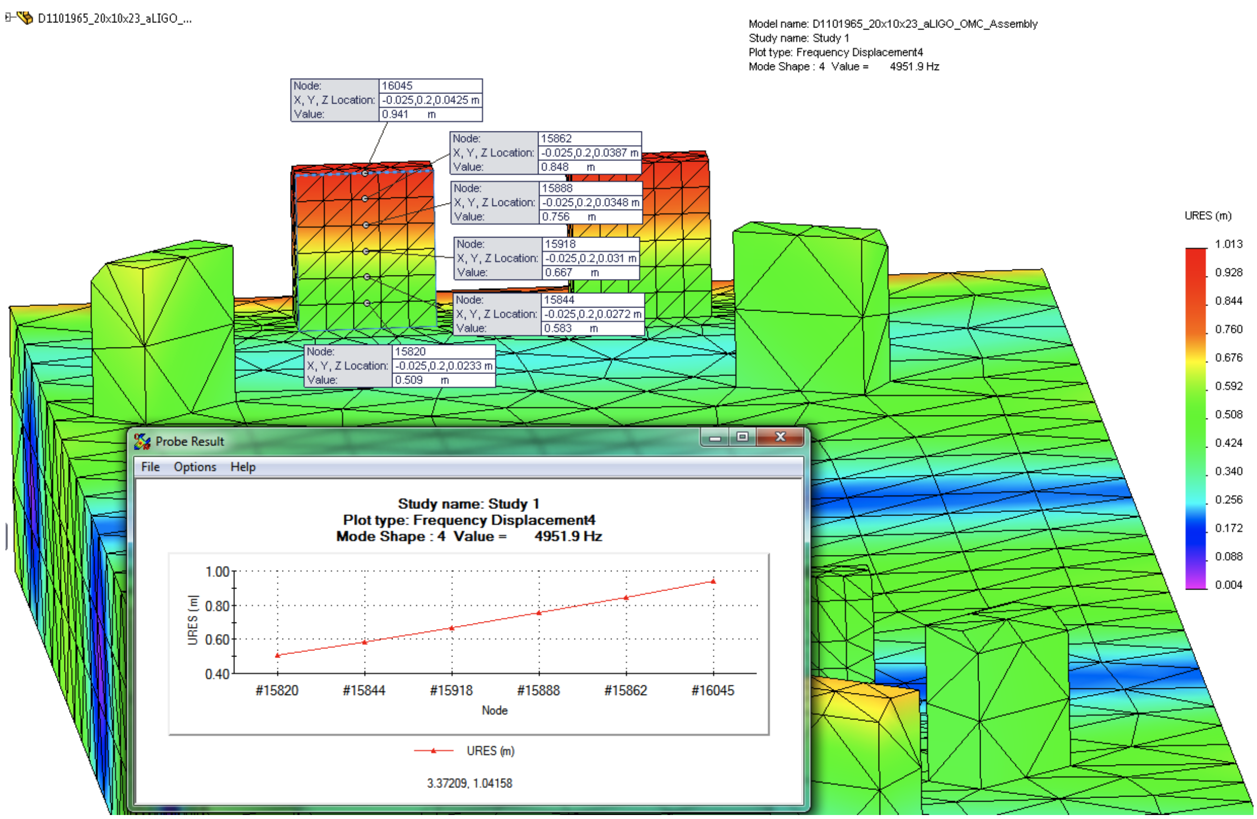


Figure 6: Example of the finite element analysis of tombstone deflection.

## 4.2 Actuators

The combined PZT and heater actuation design of the eLIGO OMC caused significant operational problems. Since then, we have identified a long-throw, multi-layer PZT stack from

Noliac[1] that achieves several micron range from a very small, few millimeter thick package. In addition to removing the heater from the design, we will mount the curved mirrors using their back surfaces instead of the front. While placing additional demands on the assembly and mirror specification, this technique should reduce the scatter and loss associated with glue on the mirror front surface.

### 4.3 OMC suspension interface

The eLIGO OMC was suspended with the wire break offs 3 mm above the center of gravity. This led to an awkward mounting interface. Using a suspension model from Mark Barton, we calculated the effect of shifting the mounting point upwards to 5 cm, such that the wires could connect to the "dark side" of the OMC. The effect on frequencies is tabulated in Table 3.

| 3 mm | | 5 cm | |
|---|---|---|---|
| Freq. [Hz] | ID | Freq. [Hz] | ID |
| 0.48 | yaw2,yaw1 | 0.48 | yaw2,yaw1 |
| 0.71 | pitch2,pitch1 | 0.70 | pitch2,pitch1 |
| 0.72 | roll2,roll1 | 0.70 | roll2,roll1 |
| 0.75 | roll2,roll1 | 1.09 | roll2,roll1 |
| 0.80 | pitch2,pitch1 | 1.12 | z2,z1 |
| 1.12 | z2,z1 | 2.12 | pitch1,pitch2 |
| 2.55 | y1 | 2.56 | y1,roll1 |
| 2.55 | x1 | 2.78 | pitch1 |
| 3.60 | yaw1 | 3.60 | yaw1 |
| 3.92 | pitch1 | 4.03 | pitch1 |
| 4.48 | z1 | 4.48 | z1 |

Table 3: The effect of shifting the suspensions point from 3 mm above the C.G. to 5 cm.

An example of the new mounting scheme is shown in Figure 7.

[1] www.noliac.com, eg. CMAR04 ID=9 mm, OD=15 mm ring with 2.8$\mu m$ stroke.

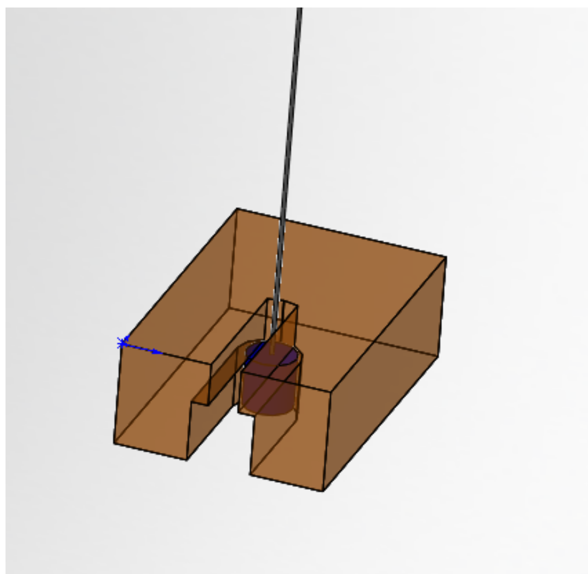

Figure 7: The proposed "Dark side" mounting scheme.

# 5 HAM6 Layout

Finally, we consider the HAM6 layout using the designs above. The mode matching telescope was designed by Keita in Ref. [3]. In addition to the OMC, the HAM6 chamber includes:

**Tip/Tilts** TT1 thru TT3 provide mode matching for the AS beam, with TT1 and TT2 providing beam steering and stabilization.

**AS-C** A quadrant photodiode in transmission of TT1, used to control the beam spot at the SRM and to trigger the fast shutter

**Fast Shutter** Triggered by AS-C, closes in 1 ms or less to protect the OMC and wave front sensor diodes

**AS wavefront sensors** Two RF wavefront sensors in transmission of TT3 provide global alignment signals

**OMC Reflection QPDs** Two DC QPDs in reflection from the OMC may provide alignment signals

**Beam diverters** Two (maybe three) beam diverters can redirect the in-air monitor beams.

The layout is similar for both OMC configurations.

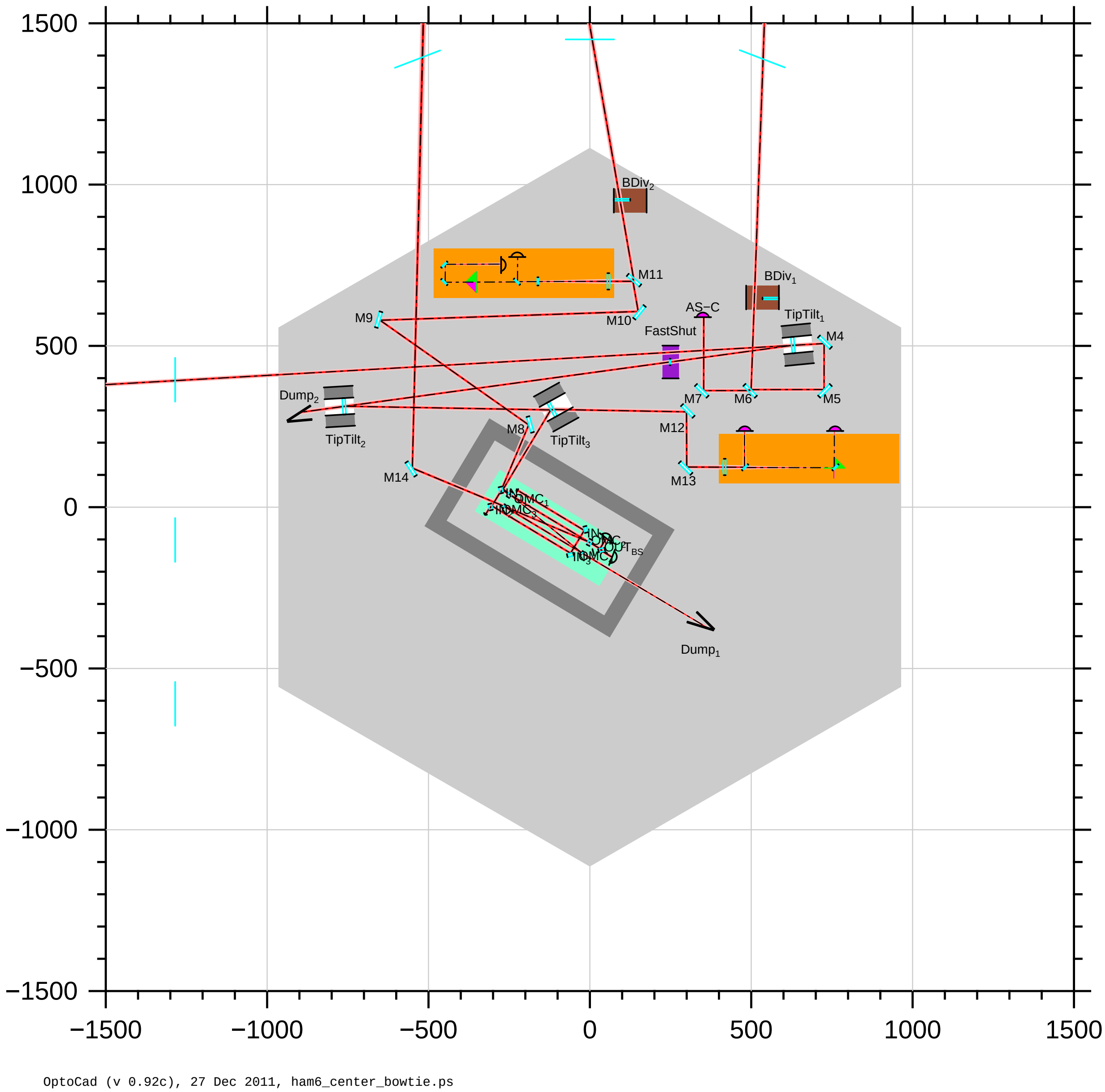


Figure 8: The HAM6 layout.